J Math Chem (2010) 48:508–520
DOI 10.1007/s10910-010-9687-1

ORIGINAL PAPER

Identification of unknown diffusion coefficient in pure diffusive linear model of chronoamperometry. II. Numerical implementation

Alemdar Hasanov · Burhan Pektaş

Received: 4 March 2009 / Accepted: 21 April 2010 / Published online: 5 May 2010

Abstract This article presents numerical implementation of the approach proposed in the previous study (*Identification of the unknown diffusion coefficient in ion transport problem. I. The theory, Math. Chem.* (2009) (submitted)) for the coefficient inverse problems related to linear diffusion equation in chronoamperometry. The coarse-fine grid algorithm is used for determination of the unknown diffusion coefficient $D(x)$ in the linear parabolic equation $u_t = (D(x)u_x)_x$ from the measured output data (left flux). The main distinguished feature of the implemented algorithm is the use of a fine grid for the numerical solution of well-posed forward and backward parabolic problems, and a coarse grid for the interpolation of the unknown diffusion coefficient $D(x)$. The nodal values of the unknown coefficient on the coarse grid are recovered sequentially, solving on each step of the coarse grid iteration algorithm the well-posed forward, and the sequence of backward pababolic problems. This guarantees a compromise between the accuracy and stability of the solution of the considered inverse problem. An efficiency and applicability of the proposed approach is demonstrated on various numerical examples with noisy free and noisy data.

Keywords Unknown diffusion coefficient · Coefficient identification · Coarse-fine grid algorithm · Noisy data

1 Introduction

We consider the inverse problem of determining the unknown coefficient $D(x)$ in the diffusion equation:

A. Hasanov (✉) · B. Pektaş
Department of Mathematics and Computer Science, Izmir University, 35140 Uckuyular, Izmir, Turkey
e-mail: alemdar.hasanoglu@gmail.com

$$\begin{cases} u_t(x,t) = (D(x)u_x(x,t))_x, \quad (x,t) \in \Omega_T := \left\{(x,t) \in R^2 : \ 0 < x < L, \ 0 < t \le T\right\}, \\ u(x,0) = 0, \quad x > 0, \\ u(0,t) = u_0/z_r, \quad u(L,t) = 0, \quad t \in (0,T] \end{cases} \tag{1}$$

from the Neumann type *measured output data* (left flux)

$$\varphi_l(t) := -D(0)u_x(0,t), \quad t > 0. \tag{2}$$

Here the functions $u(x,t)$ and $D(x)$ are defined to be the concentration of reduced species and the diffusion coefficient. $u_0 > 0$ is the initial concentration at the electrode and z_r is the valence of the reduced species. The function $\varphi_l(t)$ represents the flux at the electrode surface and is assumed to be the *measured output data*. In this context the parabolic problem (1) will be referred as a *direct (forward) problem*, with the *inputs* u_0, z_r and $D(x)$.

Let $u = u(x,t;D)$ be the solution of the direct problem (1), corresponding to the given coefficient $D(x)$. Then the function $\varphi_{ls}(t) := -D(0)u_x(0,t;D)$ will be defined as the *synthetic output data* [1,2].

Most widely used methods for identifying the unknown diffusion coefficient from the measured output data are defined to be output least squares (OLS) [3–5]. Here the measured over specifications are used to define an error functional by using an appropriate norm. An approximate solution of the inverse problem (1, 2) is then defined as a solution of a minimization problem for this functional over the set of admissible coefficients. Since the relationship between the inputs and outputs is expressed only indirectly through the solver, general information about the input-output mapping is not readily available by OLS methods.

The second class of methods for the coefficient identification problem is defined to be an equation error method [6–8]. Here the measured overspecifications are used as input to the differential equation in the direct problem, and then this problem is reformulated as an equation with respect to the unknown coefficient $D(x)$. This equation expresses a direct relationship between the values of the unknown coefficient and measured data. Since this relationship is problem dependent and frequently quite complicated, it is not easy find out from it properties of the input-output mappings.

The adjoint problem approach, proposed in [2,9–12] for the coefficient identification problems related to linear and nonlinear parabolic equations, is based on appropriate adjoint problems corresponding to a given direct problem. In each case of boundary conditions different integral relationships can be obtained between the solution of the direct and adjoint problems. These relationships, first of all, permit one to derive the gradient $\Delta J(D)$ of the cost functional $J(D)$ as the scalar product $(u_x, \psi_x)_{L_2[0,T]}$ of the gradients $u_x(x,t)$ and $\psi_x(x,t)$ of solutions of the direct and adjoint problems (see, [1], formula (31)). On the other hand, the obtained integral identities allow to prove the monotonicity and then invertibility of the input-output mapping. Further analysis show that these integral relationships also compose the computational framework of the coefficient identification problems.

In this paper the numerical implementation of the adjoint problem approach is presented for the inverse coefficient problem related to the pure diffusive model of chronoamperometry. It is shown that the integral identitiy, relating the direct problem

(1) and the corresponding adjoint problem becomes important tool for the numerical solution of the inverse problem of determining the unknown coefficient $D(x)$. Since the considered inverse problem is severely ill-conditioned, a coarse grid is used for interpolation of the unknown diffusion coefficient $D(x)$ to achieve the stability of the numerical solution. At the same time, fine grid is used to increase an accuracy of the direct/adjoint problems solutions. Thus modifying the coarse-fine grid algorithm, given in [2], an effective compromise between the accuracy and stability of the inverse problem is demonstrated.

The paper is organized as follows. In Sect. 2 discretization of the integral identitiy, relating the direct problem (1) and the corresponding adjoint problem, is given. Ill-conditioned nature of the inverse problem with outlines of the coarse-fine grid algorithm are described in Sect. 3. Numerical test examples with synthetic output data are presented in Sect. 4. Computational experiments related to identification of the unknown diffusion coefficient and numerical results for noise free and noisy output data are given in the final Sect. 5.

2 Discretization of the integral identitiy relating the direct and adjoint problems

Let $u_1 = u(x,t;D_1)$ and $u_2 = u(x,t;D_2)$ be two solutions of the direct problem (1) corresponding to the given coefficients $D_1(x)$ and $D_2(x)$, with $\Delta D(x) = D_1(x) - D_2(x)$. Then the synthetic output data $\varphi_{ls}^{(j)}(t) := -D_j(0)u_x(0,t;D_j)$, $j = 1,2$, corresponding to these solutions, satisfy the following integral identity [1]:

$$\int\int_{\Omega_\tau} \Delta D(x)u_{2x}(x,t)\psi_x(x,t)\mathrm{d}x\mathrm{d}t = \int_0^\tau p(t)\Delta\varphi^o(t)\mathrm{d}t, \quad \tau \in (0,T], \tag{3}$$

where $\Delta\varphi_{ls}(t) = \varphi_{ls}^{(1)}(t) - \varphi_{ls}^{(2)}(t)$, and the function $\psi(x,t) = \psi(x,t;p)$ is the solution of the adjoint problem

$$\begin{cases} \psi_t + (D_1(x)\psi_x)_x = 0, \quad (x,t) \in \Omega_\tau := \{(x,t) \in (0,L) \times [0,\tau)\}, \\ \psi(x,\tau) = 0, \quad x \in (0,L), \\ \psi(0,t) = p(t), \quad \psi(L,t) = 0, \quad t \in [0,\tau), \end{cases} \tag{4}$$

with arbitrary Dirichlet data $p(t) \in L_2[0,\tau)$, which will be defined below.

Evidently the backward parabolic problem (4) is a well-posed one, which can be easily verified by the change of time variable $\eta = \tau - t$.

For the discretization of the integral Eq. (3) with respect to the unknown coefficient $D(x)$, the following piecewise-linear approximation

$$D_I(x) = D_0(x) + \sum_{m=1}^{N_c} d_m\lambda_m(x), \quad 0 \le x \le L \tag{5}$$

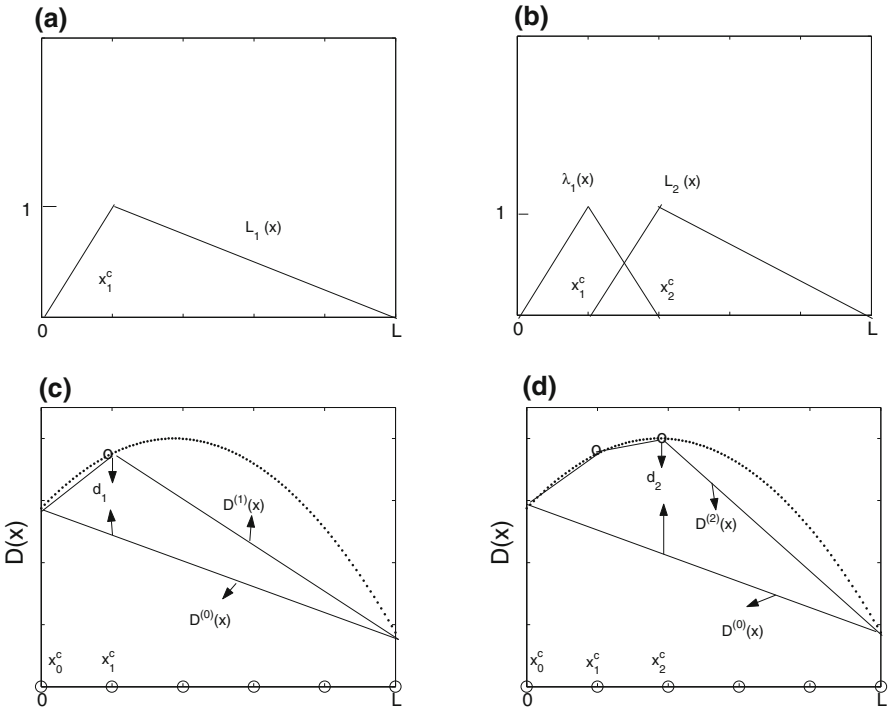

Fig. 1 Coarse grid approximation of the unknown coefficient $D(x)$

is proposed on the coarse space grid $\overline{W}_H := \left\{x_m^c \in [0, L] : \; x_0^c = 0, \; x_m^c = mh_c, \; m = \overline{1, N_c + 1}, \; h_c = L/(N_c + 1)\right\}$. Here

$$\lambda_m(x) = \begin{cases} \left(x - x_{m-1}^c\right) / \left(x_m^c - x_{m-1}^c\right), & x \in \left[x_{m-1}^c, x_m^c\right], \\ \left(x_{m+1}^c - x\right) / \left(x_{m+1}^c - x_m^c\right), & x \in \left[x_m^c, x_{m+1}^c\right], \\ 0, & x \notin \left[x_{m-1}^c, x_{m+1}^c\right], \quad m = \overline{1, N_c} \end{cases}$$

is the "fine" Lagrange type of piecewise-linear functions (Fig. 1b).

The function $D^{(0)}(x) = (1 - x/L)D(0) + (D(L)/L)x, x \in [0, L]$ is the linear polynomial, defined by the values $D(0)$ and $D(1)$ of the coefficient. These values can be defined via the the Green functions for the parabolic equations $u_t = D(0)u_{xx}$ and $u_t = D(L)u_{xx}$ [2].

The parameters d_m in (5) are defined to be the difference between the values of the interpolant $D_I(x)$ and the linear function $D^{(0)}(x)$ at the coarse grid points $x_m^c \in W_{h_c}$: $d_m = D_I\left(x_m^c\right) - D^{(0)}\left(x_m^c\right), m = \overline{1, N_c}$.

Since integral Eq. (3) is a nonlinear one, the interpolant $D_I(x)$ will be reconstructed by the iteration process, which will be organized starting from the first coarse grid point x_1^c, as follows:

$$D^{(m)}(x) = D^{(0)}(x) + \sum_{l=1}^{m-1} d_l \lambda_l(x) + d_m L_m(x), \quad 0 \le x \le L, \quad m = \overline{1, N_c}. \quad (6)$$

Here

$$L_m(x) = \begin{cases} \left(x - x_{m-1}^c\right) / \left(x_m^c - x_{m-1}^c\right), & x \in \left[x_{m-1}^c, x_m^c\right], \\ (L - x) / \left(L - x_m^c\right), & x \in \left[x_m^c, L\right], \\ 0, & x \in \left[0, x_{m-1}^c\right], \quad m = \overline{1, N_c} \end{cases}$$

is the "coarse" Lagrange type piecewise-linear functions (Fig. 1a, b). To see the role of these functions, let us assume $m = 1$ in (6). Then we have:

$$D^{(1)}(x) = D^{(0)}(x) + d_1 L_1(x), \quad 0 \le x \le L.$$

Substituting here $x = x_1^c$ and taking into account $L_1(x_1^c) = 1$ we obtain: $d_1 = D^{(1)}(x_1^c) - D^{(0)}(x_1^c)$. By the same way we may conclude that $d_m = D^{(m)}(x_m^c) - D^{(0)}(x_m^c)$. Hence the parameter d_m, $m = 1, 2, \ldots, N_c$ means the difference between the values of the mth iteration $D^{(m)}(x)$ and the initial iteration $D^{(0)}(x)$ at the coarse grid point $x_m^c \in W_{h_c}$. This iteration process is defined to be the *coarse grid iteration process*. Since $\lambda_{N_c}(x) = L_{N_c}(x)$, as a result of applying N_c times the coarse grid iteration process the piecewise linear approximation $D_I(x) := D^{(N_c)}(x)$ of the unknown coefficient $D(x)$ will be obtained in the form of interpolant (5).

3 Ill-posedness of the inverse problem. The coarse-fine grid algorithm

It is well-known that coefficient inverse problems for parabolic equations are severely ill-posed ones (see, [2] and references therein). To illustrate this distingushed feature of the considered inverse problem consider the following example. Figure 2 illustrates the two synthetic output data $\varphi_i^o(t) := D_i(0) u_{ix}(0, t; D_i)$, $i = 1, 2$ corresponding to the different diffusion coefficients $D_1(x) = 10 + (x - 1)^2$ and $D_2(x) = 20 + (x - 1)^2$. Although these output data are very close, the corresponding diffusion coefficients $D_i(x)$ are different enough. This result illustrates severely ill-conditionedness of the considered coefficient inverse problem. In particular, this implies the necessity of the use of a coarse grid for approximation of the unknown diffusion coefficient.

The integral identity (3) will be used at each mth step of the coarse grid iteration process. According to this iteration process the function $D^{(m-1)}(x)$ is assumed to be known at mth step. Hence assuming $D^{(m)}(x)$ and $D^{(m-1)}(x)$ in (3), instead of $D_1(x)$ and $D_2(x)$, accordingly, we get:

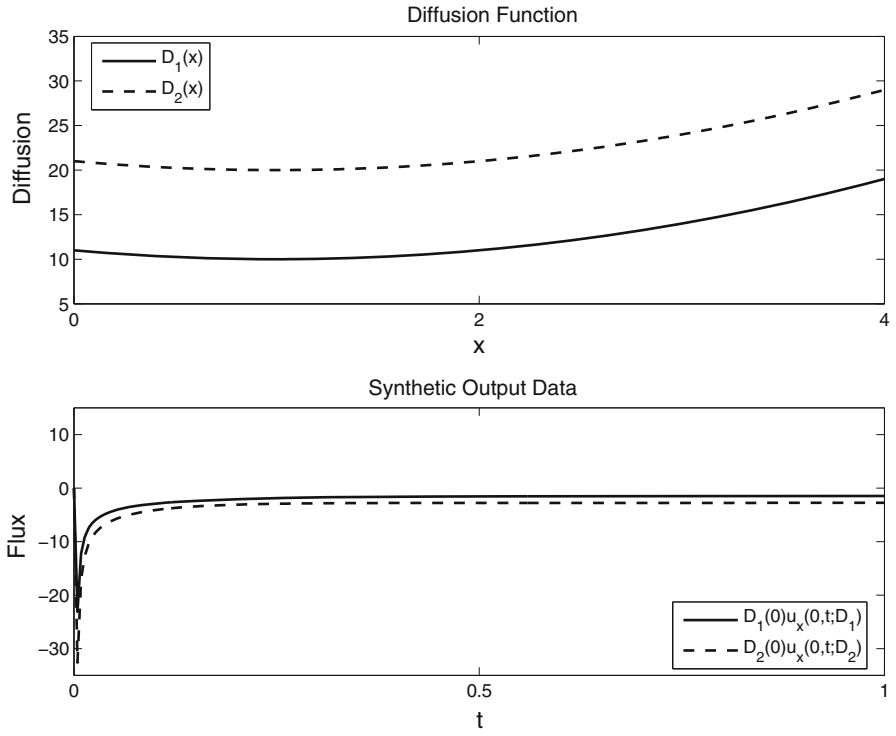

Fig. 2 Ill-posedness of the inverse problem: two close synthetic output data $\varphi_{ls}^{(i)}(t) := D_i(0)u_{ix}(0, t; D_i), i = 1, 2$, correspond to different diffusion coefficients $D_i(x)$

$$\int\int_{\Omega_{\tau_m^c}} \Delta D^{(m)}(x) u_x\left(x, t; D^{(m-1)}\right) \psi_x\left(x, t; D^{(m)}\right) \mathrm{d}x\mathrm{d}t = \int_0^{\tau_m^c} p_m(t) \Delta\varphi_{ls}^{(m)}(t)\mathrm{d}t, \tag{7}$$

where $u\left(x, t; D^{(m)}\right)$ is the solution of the direct problem (1) corresponding to the coefficient $D^{(m)}(x)$, $\Delta D^{(m)}(x) = D^{(m)}(x) - D^{(m-1)}(x)$ and $\Delta\varphi_{ls}^{(m)}(t) = \varphi_{ls}^{(m)}(t) - \varphi_{ls}^{(m-1)}(t)$, $\varphi_{ls}^{(m)}(t) = -D^{(m)}(0)u_x\left(0, t; D^{(m)}\right)$.

Equation (7) is a nonlinear integro-differential equation with respect to the unknown function $D^{(m)}(x)$. The final time $\tau = \tau_m^c$ here is taken to be the grid point of the uniform coarse time grid

$$\overline{W}_{\mathcal{T}_c} := \left\{\tau_m^c \in (0, T] : \ \tau_0^c = 0, \ \tau_m^c = m\mathcal{T}_c, \ \ m = \overline{1, N_c + 1}, \ \ \mathcal{T}_c = T/(N_c + 1)\right\},$$

which has the same number of points with the coarse space grid $\overline{W}_{h_c}$. The function $\psi\left(x, t; D^{(m)}\right)$ on the left hand side of (7) is the solution of the following adjoint problem

$$\begin{cases} \psi_t + (D^{(m)}(x)\psi_x)_x = 0, \quad (x,t) \in (0,L) \times [0, \tau_m^c), \\ \psi(x,\tau) = 0, \quad x \in (0,L), \\ \psi(0,t) = p_m(t), \quad \psi(L,t) = 0, \quad t \in [0, \tau_m^c), \end{cases} \tag{8}$$

with

$$p_m(t) = \begin{cases} 1, & 0 \le t \le \tau_{m-1}^c, \\ \left(\tau_m^c - t\right) / \left(\tau_m^c - \tau_{m-1}^c\right), & \tau_{m-1}^c \le t \le \tau_m^c. \end{cases}$$

We require that the function $D^{(m)}(x)$ (i.e. the mth iteration) is the solution of the inverse problem (1,2), which means $D^{(m)}(0)u\left(0,t;D^{(m)}\right) = \varphi(t)$, i.e. the output data $\varphi_{ls}^{(m)}(t) := D^{(m)}(0)u\left(0,t;D^{(m)}\right)$ corresponding to mth iteration coincides with the measured output data $\varphi(t)$. This requirement implies that $\Delta\varphi_{ls}^{(m)}(t) = \varphi_l(t) - \varphi_{ls}^{(m-1)}(t)$ in the integral Eq. (7), where $\varphi_l(t)$ is the noise free measured output data.

Let us transform now the nonlinear Eq. (7). Taking into account (6) we may rewrite the term $\Delta D^{(m)}(x) = D^{(m)}(x) - D^{(m-1)}(x)$ in the form $\Delta D^{(m)}(x) = [\lambda_{m-1}(x) - L_{m-1}(x)]d_{m-1} + L_m(x)d_m, m = 2,3,\ldots,N_c$. Note that for $m = 1, \Delta D_1(x) = d_1 L_1(x)$. Substituting this in (7) we obtain the following nonlinear algebraic equation with respect to the unknown parameter d_m:

$$\mathcal{M}_m(d_m)d_m + \mathcal{N}_m(d_m) = l_m, \quad m = 1,2,\ldots,N_c. \tag{9}$$

Here the nonlinear functionals $\mathcal{M}_m = \mathcal{M}_m(d_m), \mathcal{N}_m = \mathcal{N}_m(d_m)$ and the right hand side l_m are defined by the following integrals:

$$\begin{cases} \mathcal{M}_m(d_m) = \int\limits_0^{\tau_m^c}\int\limits_0^L L_m(x)u_x\left(x,t;D^{(m-1)}\right)\psi_x\left(x,t;D^{(m)}\right)\mathrm{d}x\mathrm{d}t, \\ \mathcal{N}_m(d_m) = d_{m-1}\int\limits_0^{\tau_m^c}\int\limits_0^L [\lambda_{m-1}(x) - L_{m-1}(x)]u_x\left(x,t;D^{(m-1)}\right)\psi_x\left(x,t;D^{(m)}\right)\mathrm{d}x\mathrm{d}t, \\ l_m = \int\limits_0^{\tau_m^c} p_m(t)\Delta\varphi_{ls}^{(m)}(t)\mathrm{d}t. \end{cases} \tag{10}$$

Therefore, at the mth step of the coarse grid iteration process, one needs to solve the nonlinear Eq. (9) in the domain $\Omega_{\tau_m^c} := (0,L) \times (0,\tau_m^c]$, with respect to the unknown parameter d_m. Due to nonlinearity of this equation, the series of adjoint problems (8) needs to be solved at each iteration, as the term $\psi_x\left(x,t;D^{(m)}\right)$ in (10) shows. At the same time, the term $u_x\left(x,t;D^{(m-1)}\right)$ in (10) shows that at each step of the coarse grid iteration process the forward problem (1), with already found coefficient $D^{(m-1)}(x)$ needs to be solved in $\Omega_{\tau_m^c}$ only once. For the numerical solution of the both parabolic problems we introduce the following uniform fine space $w_h := \cup_m w_h^{(m)}$ and time $w_\tau := \cup_m w_\tau^{(m)}$ grids, with the grid points $x_i^f \in w_h, \tau_j^f \in w_\tau$ and the grid steps $h_f = \left(x_{m+1}^c - x_m^c\right)/(N-1), \tau_f = \left(\tau_{m+1}^c - \tau_m^c\right)/(M-1)$, respectively. These grids consist of the following uniform sub-grids (Fig. 3)

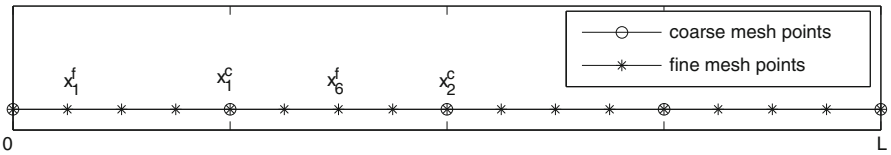

Fig. 3 The geometry of the coarse-fine space meshes

$$w_h^{(m)} := \left\{ x_i^f \in \left[x_m^c, x_{m+1}^c\right] : x_i^{(m)} = x_m^c + (i-1)h_f,\ i = \overline{(m-1)N, mN} \right\},$$
$$w_\tau^{(m)} := \left\{ \tau_j^f \in \left[\tau_m^c, \tau_{m+1}^c\right] : \tau_j^f = \tau_m^c + (j-1)\tau_f,\ j = \overline{(m-1)M+1, mM} \right\}.$$

The second iteration process needs to be constructed for the numerical solution of the adjoint problem (8) due to the dependence of the solution $\psi = \psi\left(x, t; D^{(m)}\right)$ on the unknown coefficient $D^{(m)}(x)$. Thus at the mth step of the coarse grid iteration process the nonlinear algebraic Eq. (9) requires the numerical solution of the forward and backward parabolic problems, on the fine grid $w_{h\tau} := w_h \times w_\tau$. This iteration process will be defined as the *fine grid iteration process*.

4 Numerical solution of the nonlinear equation (9) and synthetic output data generation

The following simple iteration algorithm is used for linearization of the the nonlinear algebraic Eq. (9):

$$\mathcal{M}_m\left(d_m^{(n-1)}\right) d_m^{(n)} + \mathcal{N}_m\left(d_m^{(n-1)}\right) = l_m, \quad m = 1, 2, \ldots, N_c\,. \tag{11}$$

Linearization (11) and formulas (10) show that the direct and adjoint problem solutions play an important role in this algorithm. Moreover, as mentioned above, due to the presence of the term $\varphi_x\left(x, t; D^{(m)}\right)$ on the right hand side of (10), the adjoint problem needs to be solved at each step of the fine grid iteration process, although the direct problem needs to be solved once. Hence an accuracy of the reconstruction of the unknown coefficient highly depends on the accuracy of the numerical solution of the adjoint problem (8).

For the numerical solution of the forward and adjoint problems the following implicit finite difference scheme is used:

$$\frac{y_i^{j+1} - y_i^j}{\tau_f} = \frac{1}{h_f}\left(\tilde{D}_{i+1}\frac{y_{i+1}^{j+1} - y_i^{j+1}}{h_f} - \tilde{D}_i\frac{y_i^{j+1} - y_{i-1}^{j+1}}{h_f}\right), \quad (x_i, t_j) \in w_{h\tau}, \tag{12}$$

where y_i^j is the approximate numerical value of $u(x_i, t_j) : y_i^j = u_h(x_i, t_j)$. Rewriting this scheme in the form

$$\tau_f \tilde{D}_i y_{i-1}^{j+1} - \left[\tau_f \left(\tilde{D}_{i+1} + \tilde{D}_i\right) + h_f^2\right] y_i^{j+1} + \tau_f \tilde{D}_{i+1} y_{i+1}^{j+1} = -h_f^2 y_i^j$$

and introducing the coefficients $a_i = \tau_f \tilde{D}_i$, $b_i = \tau_f \tilde{D}_{i+1}$, $c_i = \tau_f \left(\tilde{D}_{i+1} + \tilde{D}_i\right) + h_f^2$, we observe that the solvability conditions

$$a_i > 0, \quad b_i > 0, \quad c_i - (a_i + b_i) = h_f^2 > 0$$

hold. Here $\tilde{D}_i$ is the value $\tilde{D}(x_i)$ of the corresponding (at each iteration) interpolant of $D(x)$ at the fine grid point x_i^f. The implicit scheme (12) is stable, conservative and has an the order of approximation $O\left(h_f^2 + \tau_f\right)$ on the piecewise uniform fine grid $w_{h\tau}$ [13].

To analyze an effectiveness of the proposed approach, as well as to generate the synthetic noisy free output data (2), first we consider the forward problem (1) with the following four types of diffusion coefficients: monotone increasing/decreasing concave ($D''(x) < 0$), and monotone increasing/decreasing convex ($D''(x) > 0$) functions cases. These coefficients are taken to be $D(x) = 10 - x^2/4$, $D(x) = 20 - (x-4)^2$, $D(x) = 10 + (x-4)^2$ and $D(x) = 10 + (x-1)^2$, in the computational experiments below. The numerical values of these coefficients are plotted in Fig. 4, by the points. □

The forward problem (1), with these coefficients, and with the following physical and geometric parameters $u_0 = 1$, $z_r = 2$, $L = 4$, $T = 1$, is solved by using scheme (12). Two type of optimal fine grid parameters $\langle h_f, \tau_f \rangle = \langle 2.96 \times 10^{-2}, 4.40 \times 10^{-3} \rangle$ and $\langle h_f, \tau_f \rangle = \langle 1.78 \times 10^{-2}, 2.80 \times 10^{-3} \rangle$ are used for numerical solution of forward and adjoint problems. The synthetic output data $\varphi_{ls}(t) := -D(0)u_x(0, t; D(0))$ are generated from the numerical solutions of corresponding forward problems, with the above given coefficients. These synthetic output data are then used as a measured output data (2), for the inverse problems, for determination each of the unknown coefficients. Numerical results obtained by using the linearized Eq. (9) for the coarse grid parameters $N_c = 6$ and $N_c = 8$ are plotted in Fig. 4 (the lines $-\bullet-$ and piecewise linear broken lines $-\circ-$ lines, respectively). The results are close, as the figures show. Next increase of the coarse grid parameter N_c does not lead to essential increase of the relative error defined to be $\varepsilon_D = \|(D - D_I)/D\|_\infty$, as Table 1 shows. Here $D(x)$ and $D_I(x)$ are exact and numerically reconstructed coefficients, respectively. These results show that the accuracy of the proposed algorithm is high enough.

5 Computational results for noise free and noisy output data

Consider now the inverse problem with noise free ($\varphi_{lh}(t)$) and noisy ($\tilde{\varphi}_{lh}(t) = \varphi_{lh}(t) + \gamma\varphi_{lh}(t)$) synthetic flux data, where γ is the noise parameter. In all examples below

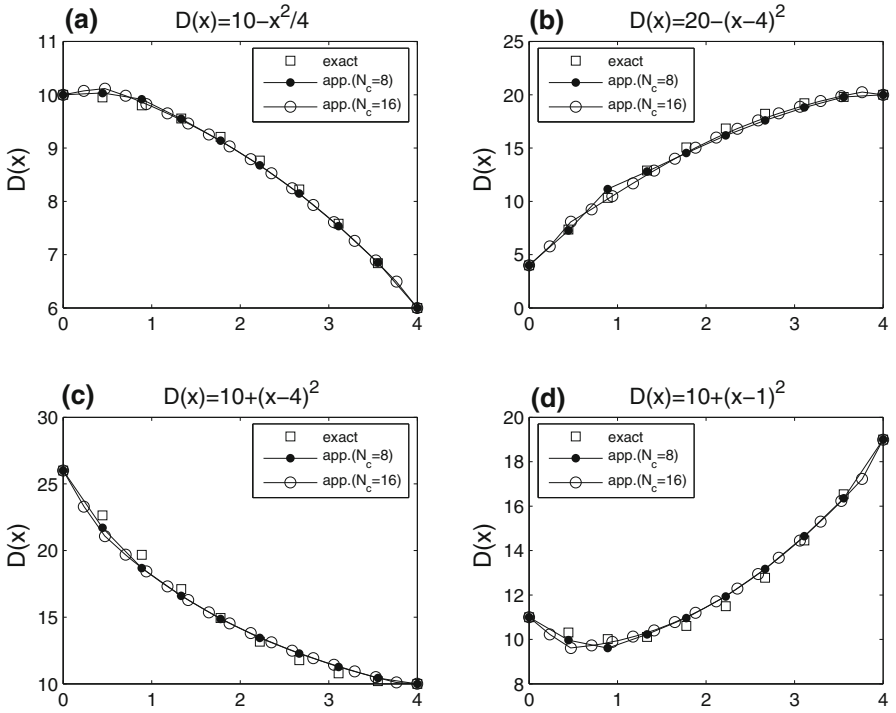

Fig. 4 Exact and reconstructed diffusion coefficients

Table 1 Relative errors ε_D corresponding to the fine and coarse grid paramaters four types of reconstructed coefficients

Fine grid parameters	$h_f = 2.96 \times 10^{-2}$ $\tau_f = 4.4 \times 10^{-3}$		$h_f = 1.78 \times 10^{-2}$ $\tau_f = 2.8 \times 10^{-3}$	
Coarse grid parameters	$N_c = 8$	$N_c = 16$	$N_c = 8$	$N_c = 16$
$D(x) = 10 - x^2/4$	1.55×10^{-2}	2.01×10^{-2}	1.18×10^{-2}	1.75×10^{-2}
$D(x) = 20 - (x-4)^2$	1.10×10^{-1}	7.85×10^{-2}	8.04×10^{-2}	6.96×10^{-2}
$D(x) = 10 + (x-4)^2$	5.68×10^{-2}	6.69×10^{-2}	5.10×10^{-2}	6.10×10^{-2}
$D(x) = 10 + (x-1)^2$	5.51×10^{-2}	7.52×10^{-2}	4.04×10^{-2}	6.50×10^{-2}

the noise free data $\varphi_{lh}(t)$ is generated from the numerical solution of the forward problem (1) for the given diffusion coefficient $D(x)$. Note that the noise free output data $\varphi_{lh}(t)$ contains a computational noise. The numerical experiments are realized for the following optimal fine grid parameters: $h_f = 2.86 \times 10^{-2}$, $\tau_f = 0.48 \times 10^{-2}$.

As a first example consider the problem of reconstruction of the strong concave coefficient $D(x) = 3 + 2\sin(0.4\pi x)$ from the noise free and noisy data, by taking the following values of the noise parameter: $\gamma = 1\%;\ 3\%$. Figure 5a illustrates the reconstructed diffusion coefficient $D(x)$ from noise free and noisy data flux data. This

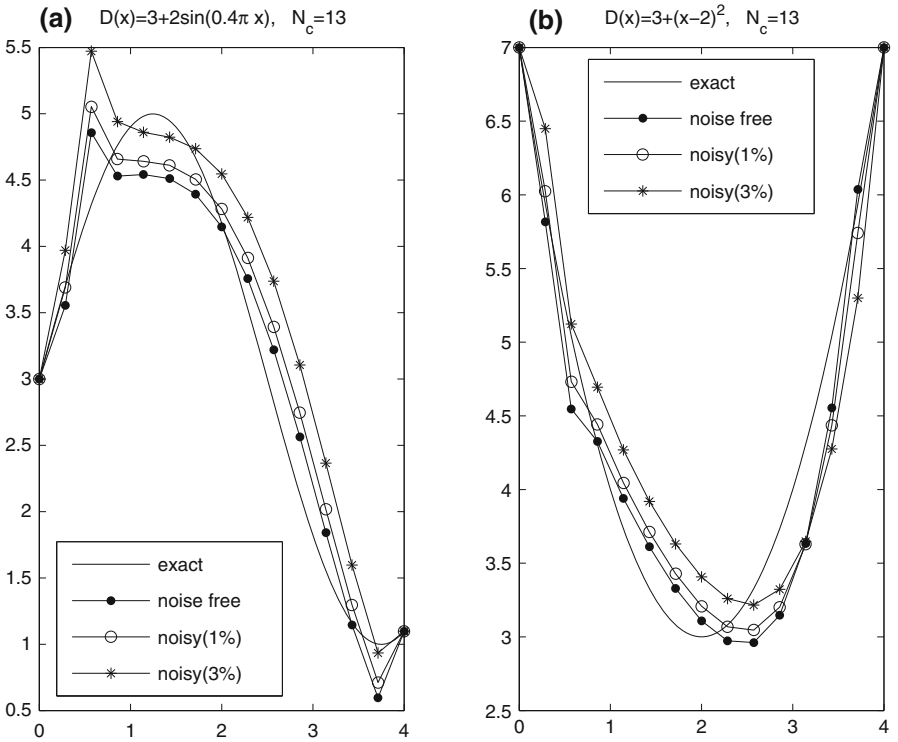

Fig. 5 Reconstruction of the concave $(D(x) = 3 + 2\sin(0.4\pi x))$ and convex $\left(D(x) = 3 + (x-2)^2\right)$ function, from the noise free and noisy flux data

Table 2 Relative errors ε_γ corresponding to the two types of reconstructed coefficients

Coefficient	Noise free	$\gamma_1 = 0.01$	$\gamma_2 = 0.03$
$D(x) = 3 + 2\sin(0.4\pi x)$	4.06×10^{-1}	2.97×10^{-1}	5.21×10^{-1}
$D(x) = 3 + (x-2)^2$	1.58×10^{-1}	1.57×10^{-1}	1.78×10^{-1}

figure also show the sensitivity of the inverse problem solution with respect to the noisy data and gradient of the reconstructed coeficient. This sensitivity can also be observed from the Table 2. Specifically, the maximum detoriation arises in the interval between the second and third coarse grid points, where the increase of the gradient $D'(x)$ is high, as Fig. 5a shows.

In the second numerical example the inverse problem of reconstruction of the convex coefficient $D(x) = 3 + (x-2)^2$ from the noise free and noisy data is considered for the same values $\gamma = 1\%;\ 3\%$ of the noise parameter. Figure 5b illustrates the reconstructed diffusion coefficient. Summarizing this and the above resulys, we may conclude that in the both cases the reconstructions are satisfactory for the values $\gamma = 1\%;\ 3\%$ of the noise parameter. Relative errors, defined to be $\varepsilon_\gamma = \|(D - D_\gamma)/D\|_\infty$, and corresponding to these cases are given in Table 2.

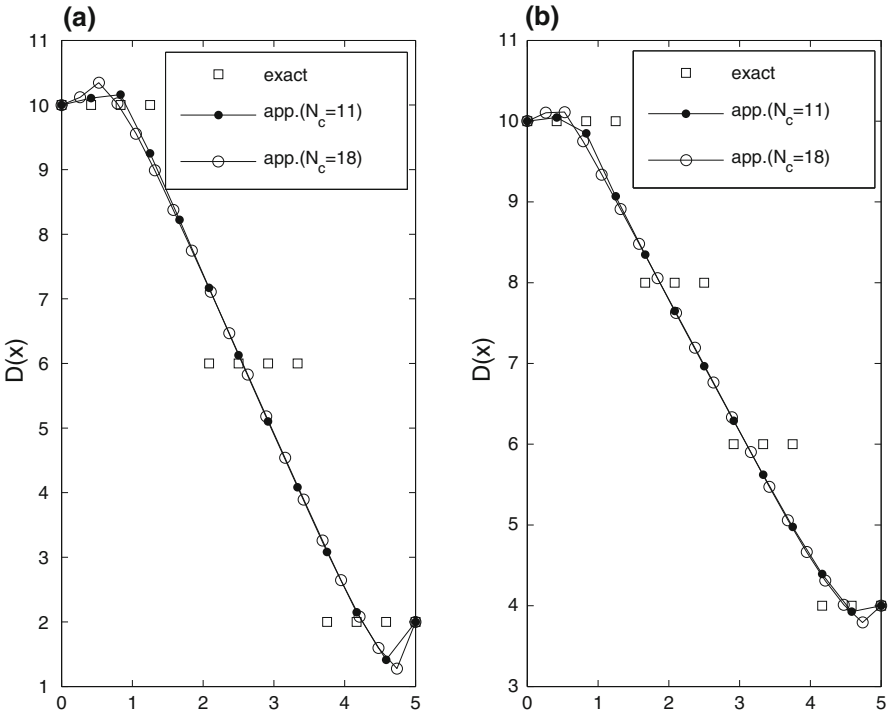

Fig. 6 Reconstruction of piecewise constant diffusion coefficients from noise free and noisy flux data

It is known that distances between closest cations and anions in lattice are quite different (see, [14]). This, in particular means that the diffusion coefficient not olny depends on the space variable $x > 0$, but also may have a character of a piecewise constant function. This case is modelled by the following two discontinuous diffusion coefficients:

$$D(x) = \begin{cases} 10, & \text{if } 0 \le x \le 1.75, \\ 6, & \text{if } 1.75 < x \le 3.5, \\ 2, & \text{if } 3.5 < x \le 5; \end{cases} \qquad D(x) = \begin{cases} 10, & \text{if } 0 \le x \le 1.25, \\ 8, & \text{if } 1.25 < x \le 2.5, \\ 6, & \text{if } 2.5 \le x \le 3.75, \\ 4, & \text{if } 3.75 < x \le 5. \end{cases} \tag{13}$$

The first function, having the jump $[D] = 4$, consists of three different constants (layered medium), and the second one, having the smaller jump $[D] = 2$, consists of four different constants. Figure 6 illustrate the reconstructed diffusion coefficients on two different coarse grids with the grid parameters $N_c = 11$ and $N_c = 18$. The relative errors corresponding to the first function are $\varepsilon_D = 5.41 \times 10^{-1}$, when $N_c = 11$, $\varepsilon_D = 6.12 \times 10^{-1}$, when $N_c = 18$, and for the second function $\varepsilon_D = 1.71 \times 10^{-1}$, when $N_c = 11$, and $\varepsilon_D = 1.67 \times 10^{-1}$, when $N_c = 18$. Hence these errors increase by increasing the jump. These results show that the proposed algorithm is also applicable for reconstruction of discontinuous diffusion coefficients.

6 Conclusion

The numerical solution of the inverse problem of determining the unknown diffusion coefficient, based on measured output (flux) data, is proposed. The algorithm of the method is based on coarse-fine grids combination, which permits one to guarantee an optimal compromise between the accuracy of the forward/adjoint problem, and stability of the severely ill-posed inverse problem. An optimal grid parameters are established for both fine and coarse grids. An efectiveness of the proposed approach is demonstrated on various computational experiments with noise free and noisy flux data. Numerical results show that the proposed algorithm is applicable for reconstruction of the diffusion coefficient not only in the class of continuous functions, but also in the class of discontinuous (piecewise constant) functions.

Acknowledgments The research has been supported by the Scientific and Technological Research Council of Turkey (TUBITAK) through the project Nr 108T332.

References

1. A. Hasanov, Math. Chem. (submitted) (2009)
2. A. Hasanov, P. DuChateau, B. Pektaş, J. Inv. Ill-Posed Prob. **14**, 435 (2006)
3. Y. Jarny, N.M. Ozisik, J.P. Bardon, Int. J. Heat Mass Transf. **34**, 2911 (1991)
4. P. Knabner, S.J. Bitterlilich, Comput. Appl. Math. **147**, 153 (2002)
5. R. Nabakov, in *Parameter Identification and Inverse Problems in Hydrology, Geology and Ecology*, ed. J. Gottlieb, P. DuChateau (Kliver Academic Publishers, Netherland, 1996), p. 155
6. M. Hanke, O. Scherzer, SIAM J. Appl. Math. **59**, 1012 (1999)
7. D.E. Reeve, M. Spivack, J. Comput. Phys. **151**, 585 (1999)
8. G.R. Richter, Math. Comput. **36**, 375 (1981)
9. P. DuChateau, SIAM J. Math. Anal. **26**, 1473 (1995)
10. P. DuChateau, in *Parameter Identification and Inverse Problems in Hydrology, Geology and Ecology*, ed. J. Gottlieb, P. DuChateau (Kliver Academic Publishers, Netherland, 1996), pp. 3–38
11. P. DuChateau, SIAM J. Math. Anal. **28**, 611 (1997)
12. P. DuChateau, R. Thelwell, G. Butters, Inverse Probl. **20**, 601 (2004)
13. A.A. Samarskii, *The Theory of Difference Schemes* (Marcel Dekker, New York, 2001)
14. J. Koryta, J. Dvořák, L. Kavan, *Principles of Electrochemistry*, 2nd edn. (Wiley, New York, 1993)